

Shadow Model Construction with Features Robust to Illumination Changes

Shuya Ishida, Shinji Fukui, Yuji Iwahori, M. K. Bhuyan, and Robert J. Woodham

Abstract—Computer vision methods need to deal with shadows explicitly because shadows often have a negative effect on the results computed. A new shadow detection method is proposed. The new method is based on a shadow model. The model is constructed by features robust to illumination changes. The method uses four features: (1) the difference of the UV components of the YUV color space between the background image and the observed image; (2) Normalized Vector Distance; (3) Peripheral Increment Sign Correlation image; and edge information. Each of these features removes shadow effects, in part. The overall method can construct an effective shadow model by using all of the features. The result is improved further by region based analysis and by online update of the shadow model. The proposed method extracts shadows accurately. Results are demonstrated by experiments using the real videos of outdoor scenes.

Index Terms—Shadow Detection, Shadow Model, Normal Vector Distance, Peripheral Increment Sign Correlation Image, Edge Information

I. INTRODUCTION

IN computer vision, detection of moving objects often is used as a preprocessing step. Many methods for detecting moving objects also detect shadows as moving objects. Accordingly, shadows can have a negative effect on the accuracy of the result. For example, there are cases where multiple objects are extracted as one object because of shadows. Methods to detect shadows and to remove them have been proposed[1]-[8].

Some methods use multiple cameras[1], [2]. These methods cannot be applied to an image obtained from a single camera. Methods using a single camera have wider application than those using multiple cameras. In this paper, a method using a single camera is developed.

Methods[3], [4] use another color space to detect shadows. Stability with respect to imaging conditions remains a problem. On the other hand, methods[5], [6], [7], [8] use shadow models. Methods[5], [6] model shadows as a mixture of distributions. These methods need to determine the number of distributions to include in the shadow model in advance. It is difficult, in general, to determine the proper number of distributions to use.

Fukui's research is supported by JSPS Grant-in-Aid for Young Scientists (B) (23700199). Iwahori's research is supported by JSPS Grant-in-Aid for Scientific Research (C)(23500228), Chubu University Grant. Woodham's research is supported by the Natural Sciences and Engineering Research Council (NSERC).

S. Ishida and Y. Iwahori are with Chubu University, Matsumoto-cho 1200, Kasugai 487-8501, Japan. e-mail: {ishida@cvl. | iwahori@}cs.chubu.ac.jp.

S. Fukui is with Aichi University of Education. e-mail: sfukui@aecc.aichi-edu.ac.jp.

M. K. Bhuyan is with Indian Inst. of Tech. Guwahati. e-mail: mkb@iitg.ernet.in

R. J. Woodham is with the University of British Columbia. e-mail: woodham@cs.ubc.ca

To address these issues, a shadow model constructed by a nonparametric Bayesian scheme was proposed[7]. The shadow model needs to be one that can be updated. Otherwise, the model will not detect shadows which are not represented in the training data. The model also should be updated only by shadow data because a suitable shadow model cannot be constructed and the method will sometimes fail to detect shadows if the training data include data which are not shadow data. A method to detect shadows and to update the shadow model was proposed[8]. That method can select the training data. Obtaining more accurate results remained as future work.

This paper proposes a new shadow model to extract shadows more accurately than the previous approaches. The new method constructs the shadow model with features robust to illumination changes: color information, Normalized Vector Distance (ND)[9], the Peripheral Increment Sign Correlation (PISC) image[10] and edge information. Each of these features can remove shadow effects, in part. The proposed method can construct an effective shadow model by using all the features. Shadow detection is improved further using object region based color segmentation. The improved result includes shadow regions which were not included in the training data. The additional shadow regions are used to update the shadow model. Results are demonstrated by experiments using real videos of outdoor scenes.

II. FEATURES ROBUST TO ILLUMINATION CHANGES

A. Normalized Vector Distance

After dividing an image into small blocks, the ND at a pixel \mathbf{x} is calculated by Eq. (1)

$$ND(\mathbf{x}) = \left| \frac{D_{\mathbf{i}}(\mathbf{x})}{|\mathbf{i}(\mathbf{x})|} - \frac{D_{\mathbf{b}}(\mathbf{x})}{|\mathbf{b}(\mathbf{x})|} \right| \quad (1)$$

where $D_{\mathbf{i}}(\mathbf{x})$ and $D_{\mathbf{b}}(\mathbf{x})$ are the irradiance data at \mathbf{x} in the observed image and the background image respectively, $\mathbf{i}(\mathbf{x})$ is the irradiance vector of the block in the observed image which includes \mathbf{x} and $\mathbf{b}(\mathbf{x})$ is that for the corresponding block in the background image.

The direction of $\mathbf{i}(\mathbf{x})$ does not change much with illumination[9]. ND is robust to illumination changes and thus can remove the effect of shadows, in part.

B. Peripheral Increment Sign Correlation

Let the sign of the difference in irradiance between \mathbf{x} and its neighbor pixel in the background image be represented by $b_i(\mathbf{x})$ ($1 \leq i \leq N$) and that for the observed image be $b'_i(\mathbf{x})$, where N is the number of neighbors considered. If the difference is less than 0, $b_i(\mathbf{x})$ is set to 0. Otherwise, it

is set to 1. Similarly, define $b'_i(\mathbf{x})$. The PISC at a pixel \mathbf{x} is a thresholded version of $B(\mathbf{x})$ where

$$B(\mathbf{x}) = \frac{1}{N} \sum_{i=1}^N (b_i(\mathbf{x})b'_i(\mathbf{x}) + (1 - b_i(\mathbf{x}))(1 - b'_i(\mathbf{x}))) \quad (2)$$

A pixel \mathbf{x} is considered an object pixel region when $B(\mathbf{x})$ is larger than a threshold. The resulting thresholded binary image is called the PISC image. Each pixel in the PISC image is 1 if the pixel is part of an object region. Otherwise, it is 0.

The sign of the difference in irradiance between \mathbf{x} and a neighbor pixel in the background region typically does not change with illumination. Thus, PISC also is a feature robust to illumination changes.

III. SHADOW MODEL

The proposed method uses three shadow models. They are described in this section.

A. Shadow Model by Color Information

The proposed method uses ND and the UV components of the YUV color space. In shadow regions, differences in the U and V components of each pixel between the background image and a target image become small. On the other hand, those in a moving object region become large. The ND also becomes small in a shadow region and large in an object region. Differences in the UV components and the ND are the observed data. The frequency distribution of the data in shadow regions is obtained and approximated as a mixture of Gaussian distributions. This is used as the shadow model.

Let the data at \mathbf{x} be represented by $\mathbf{D}_c(\mathbf{x})$. The shadow model by color information is represented by Eq. (3).

$$P_C(S(\mathbf{x})|\alpha, \theta, \mathbf{D}_c(\mathbf{x})) = \sum_{k=1}^K \alpha_k \mathcal{N}(\mathbf{D}_c(\mathbf{x}); \theta_k) \quad (3)$$

$$\alpha = \{\alpha_1, \dots, \alpha_K\}, \quad \theta = \{\theta_1, \dots, \theta_K\}$$

where $S(\mathbf{x})$ is the state that \mathbf{x} is in a shadow region, K is the number of distributions, and $\mathcal{N}(\cdot; \theta_k)$ is the k -th Gaussian distribution with parameters θ_k and mixture ratio α_k .

The parameters of the distribution are estimated by a nonparametric Bayesian scheme. The proposed method uses the DPEM algorithm[11]. DPEM is based on expectation Maximization (EM) and can be implemented easily. The algorithm calculates not only the parameters of the mixture distribution but also the mixture ratios. The DPEM algorithm can treat a probability model with a countably infinite number of distributions but the approximation is truncated to a sufficiently large finite number of distributions. The initial truncation number is set to 20 in our experiments.

After estimating the mixture ratios, the number of distributions retained in the shadow model is reduced. Distributions with small mixture ratios are removed.

B. Shadow Model by Edge Information

A method to use edge information for shadow detection has been proposed[12]. Let the differences in the edge magnitude and in the direction of the edge gradient between a current image and the background image be represented by

$E_{mag}(\mathbf{x})$ and $E_{dir}(\mathbf{x})$ respectively. The differences in the edge information for each pixel in shadow regions between the background image and a target image become small. On the other hand, those in a moving object region become large. The shadow model based on edge information is represented by Eq. (4).

$$P_E(S(\mathbf{x})|\mathbf{D}_E(\mathbf{x})) = \lambda_1 \exp(-E_{mag}(\mathbf{x})/w_1) + (1 - \lambda_1) \exp(-E_{dir}(\mathbf{x})/w_2) \quad (4)$$

$$\mathbf{D}_E(\mathbf{x}) = (E_{mag}(\mathbf{x}), E_{dir}(\mathbf{x}))$$

where λ_1 ($0 \leq \lambda_1 \leq 1$) is a relative weight and where w_1 and w_2 are parameters which tune the variances of the exponentials.

C. Shadow Model by PISC Image

Let $D_P(\mathbf{x})$ be the pixel value at \mathbf{x} in the PISC image. Here, the PISC image is constructed using normalized irradiance instead of irradiance directly. Otherwise, shadow regions tend to be extracted as object regions. A pixel which an object detection method calls an object pixel but which exists as background in the PISC image has a high probability that it is a shadow pixel. The shadow model by PISC image is represented by Eq. (5).

$$P_P(S(\mathbf{x})|D_P(\mathbf{x})) = 1 - D_P(\mathbf{x}) \quad (5)$$

IV. SHADOW DETECTION

After constructing the three shadow models, shadow detection can proceed. Shadow detection is applied to pixels selected by the object detection method. Shadow detection proceeds as follows: First, the probability that a pixel exists in a shadow region is calculated. Next, shadow regions and object regions are separated by a thresholding process. Finally, the result is refined based on the object regions obtained and on color segmentation[13]. Detection and refinement of the result are explained in the following subsections.

A. Shadow Detection using the Shadow Model

The probability that \mathbf{x} belongs to the shadow region is calculated by Eq. (6).

$$P_1(S(\mathbf{x})|\alpha, \theta, \mathbf{D}(\mathbf{x})) = P_C(S(\mathbf{x})|\alpha, \theta, \mathbf{D}_C(\mathbf{x})) \cdot P_E(S(\mathbf{x})|\mathbf{D}_E(\mathbf{x})) \cdot P_P(S(\mathbf{x})|D_P(\mathbf{x})) \quad (6)$$

$$\mathbf{D}(\mathbf{x}) = (\mathbf{D}_C(\mathbf{x}), \mathbf{D}_E(\mathbf{x}), D_P(\mathbf{x}))$$

$P_1(S(\mathbf{x})|\alpha, \theta, \mathbf{D}(\mathbf{x}))$ is large when \mathbf{x} is in a shadow region. When $P_1(S(\mathbf{x})|\alpha, \theta, \mathbf{D}(\mathbf{x}))$ is larger than a threshold \mathbf{x} is considered to be in a shadow region. Otherwise, \mathbf{x} is considered to be in an object region.

B. Refining the Shadow Detection Result

The above process will misclassify some pixels. Refinement consists of two parts. First, the pixel-level results are refined using the object regions already obtained. Second, color segmentation[13] is used to refine the results further. The two refinements are described in the following.

Let $R_{(i)}$ ($i = 1, \dots, N$) be the labeled object regions, where N is the total number of object regions. Small regions

are removed as noise. The probability that \mathbf{x} is not in an object region is calculated by the following equation.

$$P_R(S(\mathbf{x}_{(i)})|\boldsymbol{\theta}_{R_{(i)}}, \mathbf{x}_{(i)}) = 1 - \exp\left(-c\overline{\mathbf{x}}_{(i)}^\top \boldsymbol{\Sigma}_{R_{(i)}}^{-1} \overline{\mathbf{x}}_{(i)}\right) \quad (7)$$

$$\boldsymbol{\theta}_{R_{(i)}} = \left\{ \boldsymbol{\mu}_{R_{(i)}}, \boldsymbol{\Sigma}_{R_{(i)}} \right\}, \quad \overline{\mathbf{x}}_{(i)} = \mathbf{x}_{(i)} - \boldsymbol{\mu}_{R_{(i)}}$$

where $\mathbf{x}_{(i)}$ denotes a pixel with nearest object region $R_{(i)}$, $\boldsymbol{\mu}_{R_{(i)}}$ is the centroid of $R_{(i)}$, and $\boldsymbol{\Sigma}_{R_{(i)}}$ is the variance-covariance matrix of the positions of all the pixels in $R_{(i)}$.

The probability that $\mathbf{x}_{(i)}$ is in shadow, not in an object region, is calculated by Eq. (8)

$$P_2(S(\mathbf{x}_{(i)})|\boldsymbol{\alpha}, \boldsymbol{\theta}, \boldsymbol{\theta}_{R_{(i)}}, \mathbf{D}(\mathbf{x}_{(i)}), \mathbf{x}_{(i)}) = \lambda_2 P_1(S(\mathbf{x}_{(i)})|\boldsymbol{\alpha}, \boldsymbol{\theta}, \mathbf{D}(\mathbf{x}_{(i)})) \cdot P_R(S(\mathbf{x}_{(i)})|\boldsymbol{\theta}_{R_{(i)}}, \mathbf{x}_{(i)}) + (1 - \lambda_2) P_R(S(\mathbf{x}_{(i)})|\boldsymbol{\theta}_{R_{(i)}}, \mathbf{x}_{(i)}) \quad (8)$$

where λ_2 ($0 \leq \lambda_2 \leq 1$) is a relative weight. Pixel \mathbf{x} is classified as shadow or object by thresholding P_2 .

P_R becomes smaller when $\mathbf{x}_{(i)}$ is closer to $\boldsymbol{\mu}_{R_{(i)}}$. For misclassified object pixels, P_2 becomes smaller than P_1 . On the other hand, for misclassified shadow pixels, P_2 becomes larger owing to the effect of P_R . The overall result is improved through the second thresholding applied to P_2 .

Finally, Mean-Shift[13] is used for color segmentation. Any resulting color region with more than 60% of its pixels classified as shadow, based on the thresholding of P_2 , is classified entirely as shadow. Otherwise, the entire region is classified as object.

V. UPDATING THE SHADOW MODEL

The initial shadow model is trained manually with data selected from shadow regions. Subsequently, the shadow model is updated in order to detect shadows which were not included in the training data. Shadow regions detected by the process explained in the previous section are used to update the model. Updating the model proceeds as follows:

STEP 1 Obtain training data

STEP 2 Obtain initial values for DPEM

STEP 3 Update the shadow model using DPEM

STEP 1 and **STEP 2** are described further in the following sub-sections.

A. Obtain Training Data

Data from pixels detected as shadow pixels in previous frames are stored. If data of all past frames are stored, the dataset will become enormous and the DPEM algorithm will require a great deal of time to run. Furthermore, the impact of shadow data obtained in the current frame will diminish. Instead, data are stored selectively. The method to obtain training data is described as follows.

First, pixels in object regions misclassified as shadow are removed from the current shadow data. Properties of an entire object region are used to select shadow pixels deemed to be misclassified. Each object region labeled through the process described in section IV-B is considered, as follows. The variance-covariance matrix for the coordinates of the pixels in the object region is calculated and a 95% probability ellipse is obtained. All pixels inside this ellipse are

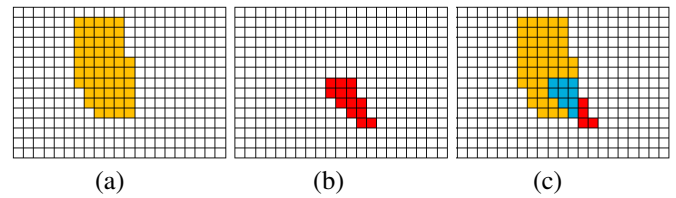


Fig. 1. Process to Update Shadow Data: (a) Pixels Having Shadow Data at Time $t - 1$, (b) Pixels in the Current Shadow Region, and (c) Pixels Having Shadow Data at Time t

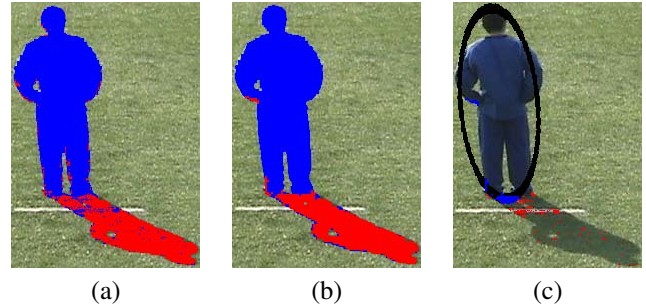


Fig. 2. Process to Detect Data not Included in Previous Training Data: (a) Result by Threshold, (b) Result by Segmentation, and (c) Data used at **STEP 2**

regarded as object pixels. Any currently considered shadow are removed from the shadow data.

Current shadow data obtained by the processes described in section IV are added to the training data. At the same time, data from pixels which were regarded as in a shadow region in past frames are overwritten. Fig. 1 illustrates this process. Data from the red pixels in Fig. 1-(c) are added to the shadow data and data from the blue pixels are overwritten by new current shadow data. This process keeps the total amount of data to manage reasonable.

B. Obtain Initial Values for DPEM

Accuracy of the result estimated by the DPEM algorithm depends on the initial values of its parameters. Parameters needed are the mean vector and the variance-covariance matrix for each Gaussian distribution. A sufficiently large number of initial distributions for truncation is also needed. The number of distributions and the initial parameters for the mixture distribution are determined by the following process.

STEP I Obtain data not included in the training data

STEP II Apply DPEM to the data obtained by **STEP I**

At **STEP I**, shadow data not included in the training data are obtained. Pixels reclassified from object region to shadow region are used. Fig. 2 shows the process for **STEP I**. Blue pixels in the figure indicate pixels regarded as object pixels and red ones indicate pixels regarded as shadow. The red pixels in Fig. 2-(c) are used as training data at **STEP II**.

At **STEP II**, the DPEM algorithm is applied to the data obtained at **STEP I**. The number of distributions for truncation is set to 20. The initial mean vector for each distribution is set to a datum obtained randomly from the data. The initial variance-covariance matrix is set to the variance-covariance matrix which is calculated from the data. After DPEM is applied, the number of distributions for the data is determined according to the resulting mixture ratios.

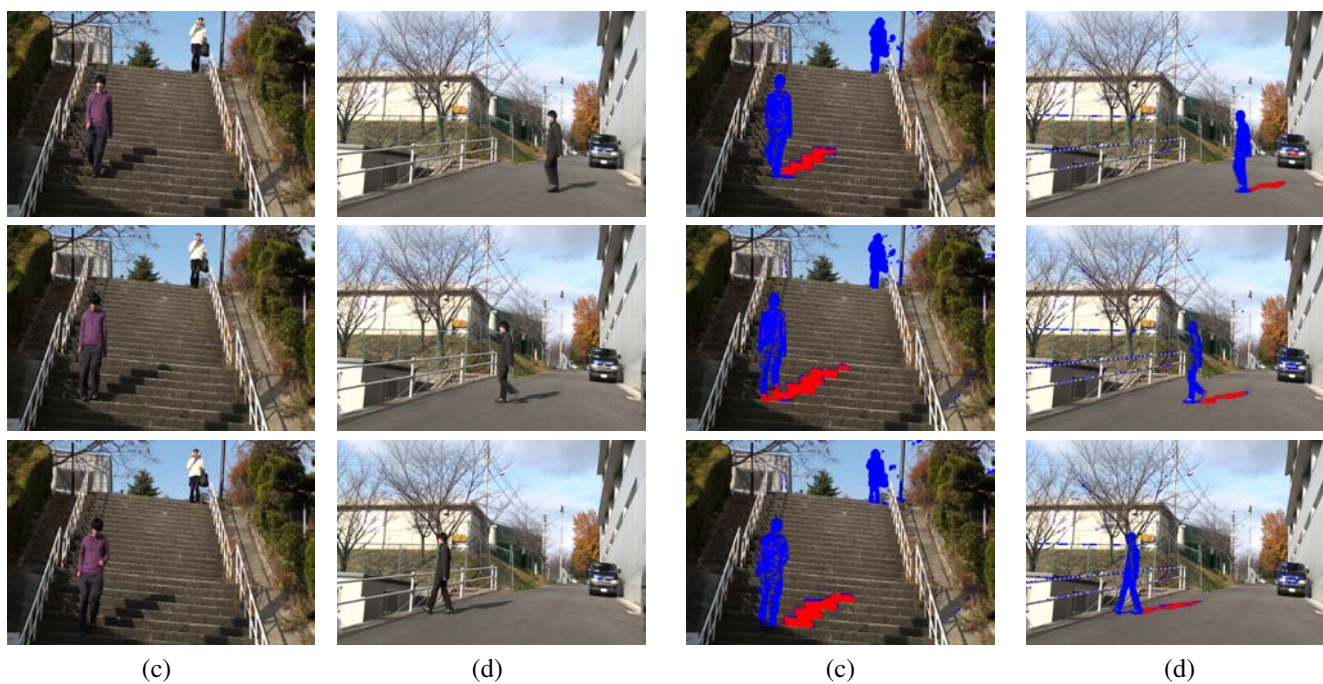
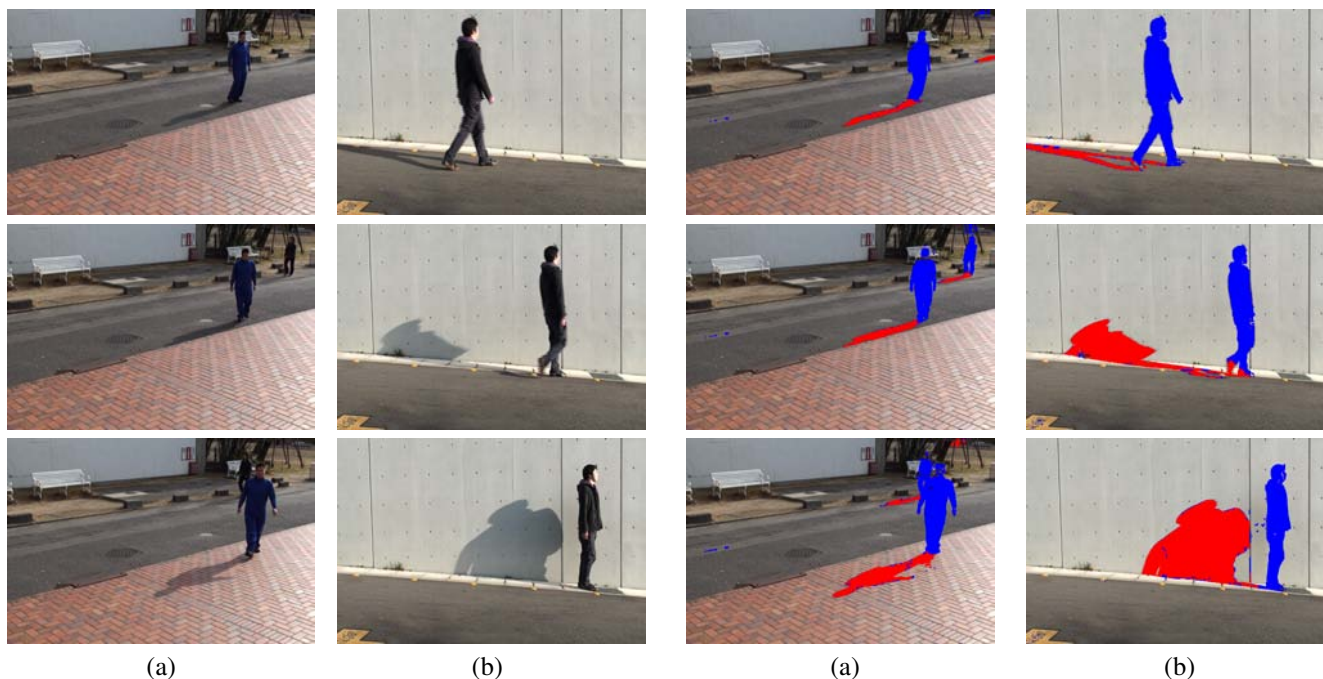


Fig. 3. Input Images: (a) Scene1, (b) Scene2, (c) Scene3 and (d) Scene4

Fig. 4. Results: (a) Scene1, (b) Scene2, (c) Scene3 and (d) Scene4

The parameters for the current shadow model and those obtained through the above process are given as the initial parameters for the DPEM algorithm. The truncation number is obtained by adding the number obtained at **STEP II** to the number of distributions for the current shadow model. Better initial parameters and a smaller truncation number result from these processes.

VI. EXPERIMENTS

Experiments using real videos of outdoor scenes were done to confirm the effectiveness of the proposed method. The size of each frame is 720×480 pixels and each pixel has an 8 bit color value for each RGB component. Four scenes (Scene1, Scene2, Scene3 and Scene4) were used in

the experiments. The proposed method was applied to the areas selected by background subtraction. Examples of input frames used in the experiments are shown in Fig. 3.

The results of shadow detection are shown in Fig. 4. Blue pixels in the figures denote object pixels and red ones denote shadow. The results show that the proposed method can detect most shadows. Pixels in the regions of the shoes are misclassified as shadow. In this case, the color of the shoes in the original image is similar to that of the shadow. Since the method uses color information to construct the shadow model, it tends to misclassify object regions similar in color to shadows.

Results of method[8] are shown in Fig. 5. It is clear that the proposed method can get better results than with method[8]. The proposed method models shadows effectively with four

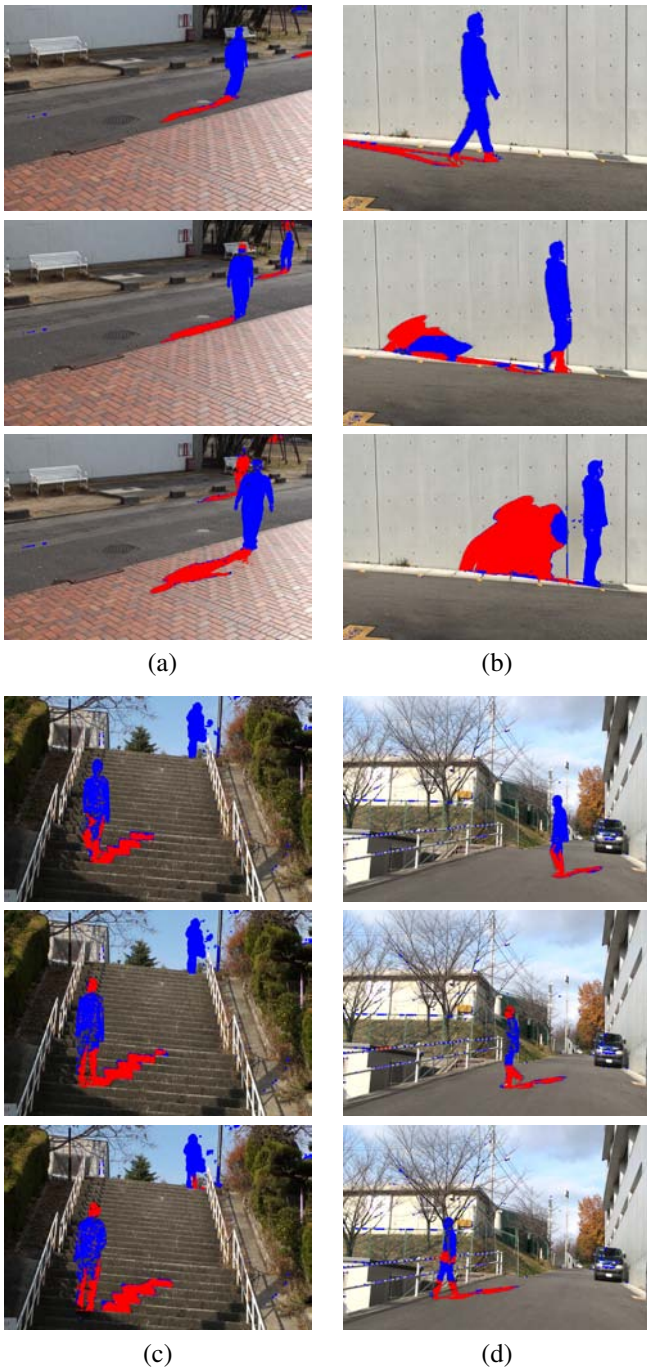


Fig. 5. Results by Method[8]: (a) Scene1, (b) Scene2, (c) Scene3 and (d) Scene4

different features.

In [14], the shadow detection rate, η , and the shadow discrimination rate, ξ , were introduced. They are calculated by Eq. (9) and Eq. (10) respectively.

$$\eta = \frac{TP_s}{TP_s + FN_s} \quad (9)$$

$$\xi = \frac{\overline{TP}_f}{\overline{TP}_f + \overline{FN}_f} \quad (10)$$

where TP is the number of true positives, FN is the number of false negatives, subscript s denotes shadow, subscript f denotes foreground and \overline{TP}_f is the difference between the correct number of points on foreground objects and the number of points on foreground objects misclassified as shadow.

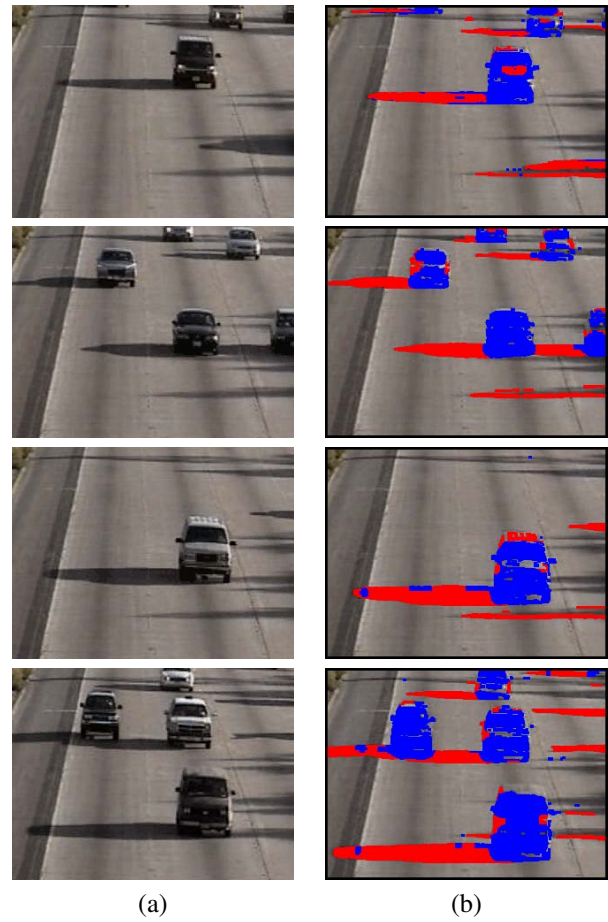


Fig. 6. Input Images and Results: (a) Input Images and (b) Results

Table I shows η and ξ for each of the four scenes comparing the proposed method and method[8]. Some of the values for the proposed method are lower than those for method[8]. The shadow detection rate, η , becomes larger when more shadow pixels occur even though many misclassified pixels exist in the object regions. Similarly, the shadow discrimination rate, ξ , becomes larger when more object pixels occur even though many misclassified pixels exist in the shadow regions. The overall result is good when both values are high. The proposed method obtains better results than the previous method[8] when η and ξ are compared simultaneously.

Four methods[15]-[18] were evaluated quantitatively in [14] based on η and ξ . One of the five videos used for that evaluation was used in this work to compare the performance of our method with the four results reported in [14].

Examples of our results are shown in Fig. 6. Table II compares η and ξ for our method with the reported results for the other four methods. The values reported for our method are averages of 100 frames in the video sequence. Values reported for the other methods were calculated over more frames. Even though the comparisons therefore are not identical, the table shows that our method estimates shadow regions with high performance, based on η and ξ .

VII. CONCLUSION

This paper has proposed a new model for shadow detection. The shadow model is constructed from color information, Normalized Vector Distance, the Peripheral Increment Sign Correlation image and edge information. These are

TABLE I
SHADOW DETECTION RATES (η) AND SHADOW DISCRIMINATION RATES (ξ) FOR FOUR SCENES

		scene1			scene2			scene3			scene4		
η [%]	Proposed Method	92.59	93.85	93.02	81.56	95.51	95.66	78.30	89.05	88.27	88.72	85.47	74.44
	Method [8]	90.06	92.33	92.52	80.65	50.25	52.33	85.16	89.25	89.71	78.85	84.76	86.53
ξ [%]	Proposed Method	96.57	98.61	95.14	99.65	99.65	99.01	99.93	94.51	99.94	98.79	99.32	99.73
	Method [8]	96.72	92.57	82.63	94.23	85.16	97.03	84.15	78.48	74.89	80.44	71.43	73.79

TABLE II
 η AND ξ FOR VIDEO USED IN [14]

	η	ξ
Proposed Method	91.56	95.68
Method[15]	81.59	63.76
Method[16]	59.59	84.70
Method[17]	69.72	76.93
Method[18]	75.49	62.38

features robust to illumination changes. Each helps to remove shadow effects, in part. A shadow model including all these features estimates shadow pixels more accurately. The results are further improved by region based analysis.

The proposed method updates the shadow model to detect shadows which were not included in the training data. The experimental results show that shadow regions are estimated more robustly than with previous approaches.

Future work will explore how to determine the parameters of the initial shadow model and shadow detection automatically and how to construct a shadow model without an explicit background image.

REFERENCES

[1] C.B. Madsen, T.B. Moeslund, A. Pal and S. Balasubramanian: "Shadow Detection in Dynamic Scenes Using Dense Stereo Information and an Outdoor Illumination Model," *Proc. of DAGM2009 Workshop on Dynamic 3D Imaging*, pp. 110–125, 2009.

[2] H. Iwama, Y. Makihara and Y. Yagi: "Foreground and Shadow Segmentation Based on a Homography-Correspondence Pair," *ACCV2010*, pp. 2790–2802, 2010.

[3] C. Grana, M. Piccardi, A. Prati and S. Sirotti: "Improving shadow suppression in moving object detection with HSV color information," *Proc. IEEE Intelligent Transportation Systems Conf.*, pp. 334–339, 2001.

[4] P. Blauensteiner, H. Wildenauer, A. Hanbury, and M. Kampel: "On colour spaces for change detection and shadow suppression," *Proc. 11th Computer Vision Winter Workshop, Telc, Czech Republic*, pp. 87–92, 2006.

[5] T. Tanaka, A. Shimada, D. Arita and R. Taniguchi: "Object detection based on non-parametric adaptive background and shadow modeling," *ACCV2007*, pp. 159–168, 2007.

[6] Y. Wang, H. Cheng and J. Shan: "Detecting shadows of moving vehicles based on HMM," *ICPR2008*, pp. 1–4, 2008.

[7] W. Kurahashi, S. Fukui, Y. Iwahori, R.J. Woodham: "Shadow Detection Method Based on Dirichlet Process Mixture Model," *LNCS*, Vol. 6278/2010 KES2010, pp. 89–96, 2010.

[8] S. Fukui, W. Kurahashi, Y. Iwahori, R.J. Woodham: "Method of Updating Shadow Model for Shadow Detection based on Nonparametric Bayesian Estimation," *IAPR Int'l Conf. on Machine Vision Application*, pp. 10–13, Jun, 2011.

[9] S. Nagaya, T. Miyatake, T. Fujita, W. Ito and H. Ueda: "Moving Object Detection by Time-Correlation-Based Background Judgement Method," in *Trans. of IEICE*, Vol. J79-D-II, No. 4, pp. 568–576, 1996. (in Japanese)

[10] Y. Sato, S. Kaneko and S. Igarashi: "Robust Object Detection and Segmentation by Peripheral Increment Sign Correlation Image," *IEICE Trans. on Info. and Sys.*, Vol. J84-D-2, No.12, pp. 2585–2594, 2001. (in Japanese)

[11] T. Kimura, Y. Nakada, A. Doucet and T. Matsumoto: "Semi-supervised learning scheme using Dirichlet process EM-algorithm," *IEICE Tech. Rep.*, 108(484):77–82, 2009.

[12] A.J. Joshi, S. Atev, O. Masoud, and N. Papanikolopoulos: "Moving Shadow Detection with Low- and Mid-Level Reasoning," *IEEE International Conference on Robotics and Automation 2007*, pp. 4827–4832, 2007.

[13] D. Comaniciu and P. Meer: "Mean Shift Analysis and Applications," *Proc. of the International Conf. on Computer Vision*, Vol.2, pp. 1197–1203, 1999.

[14] A. Prati, I. Mikic, M.M. Trivedi, and R. Cucchiara: "Detecting Moving Shadows: Algorithms and Evaluation," *IEEE Trans. on PAMI*, vol. 25, No. 7, pp. 918–923, 2003.

[15] I. Haritaoglu, D. Harwood, and L.S. Davis: "W⁴: Real-Time Surveillance of People and Their Activities," *IEEE Trans. on PAMI*, vol. 22, no. 8, pp. 809–830, Aug. 2000.

[16] I. Mikic, P. Cosman, G. Kogut, and M.M. Trivedi, "Moving Shadow and Object Detection in Traffic Scenes," *Proc. Int'l Conf. Pattern Recognition*, vol. 1, pp. 321–324, Sept. 2000.

[17] R. Cucchiara, C. Grana, G. Neri, M. Piccardi, and A. Prati: "The Sakbot System for Moving Object Detection and Tracking," *Video-Based Surveillance Systems Computer Vision and Distributed Processing*, pp. 145–157, 2001.

[18] J. Stauder, R. Mech, and J. Ostermann: "Detection of Moving Cast Shadows for Object Segmentation," *IEEE Trans. Multimedia*, vol. 1, no. 1, pp. 65–76, Mar. 1999.